Targeted Anticancer Drug Delivery Using Nanoparticles For Treatment of Colon Cancer

Dolly Jain*, Deshraj Chumbhale
*Faculty of Pharmacy, Oriental University, Indore, 453555, Madhya Pradesh, India

Corresponding Author*
Dolly Jain
Email: dollyjain.btpc@gmail.com
DOI: 10.31838/ecb/2023.12.si7.310

Abstract

This research study aimed to enhance the therapeutic potential of the drug Doxorubicin (DX) by incorporating it into PL NPs and HyAc/PEG/PL NPs, (nanoparticle composed of hyaluronic acid, polyethylene glycol, and polycaprolactone) while optimizing their composition. The developed NPs were utilized to encapsulate DX and subsequently subjected different evaluation parameters including evaluation of surface morphology, DSC, XRD, entrapment efficiency), in vitro drug release, hemolytic toxicity, tissue distribution study, cell viability, and stability. The nanoparticles exhibited a spherical shape as observed through TEM examinations. The zeta potential measurements for HyAc/PEG/PL NPs and PL NPs were determined to be 16.4±0.84 mV and -4.9±0.3 mV, respectively, with corresponding PDI values of 0.648 and 0.553 for both formulations. The particle sizes of HyAc/PEG/PL NPs and PL NPs were found to be 268±3nm and 142±1.5nm, respectively. The NPs exhibited sustained release of DX, with DX-loaded HyAc/PEG/PL NPs releasing a significant amount of DX over a period of 96 hours, while DX-loaded PL NPs achieved nearly complete drug release within the same time frame. Evaluation of stability based on residual drug content indicated that the NPs formulations remained more stable at temperatures of 4±2°C and subsequently at 28±2°C. The hemolytic toxicity assay demonstrated the high hemocompatibility of DX-loaded HyAc/PEG/PL NPs. Moreover, biodistribution analysis revealed higher concentrations of DX in the colon and tumor when delivered using DX-loaded HyAc/PEG/PL NPs, suggesting enhanced targeting ability. Notably, due to the affinity of HyAc for over expressed CD44 receptors on HT-29 cells, the DX-loaded HyAc/PEG/PL NPs demonstrated superior cytotoxicity, indicating enhanced internalization of the formulated drug.

Keywords: Biodegradable Polymer; Cell Viability; Colorectal Cancer; Drug Delivery; Doxorubicin.

1. Introduction

In the United States, colorectal cancer (CRC) ranks as the third most frequently detected cancer and the third primary contributor to cancer-related mortality in both males and females. However, it ranks second in terms of overall cancer-related deaths and is the primary cause among men under the age of 50. It is projected that in 2023, approximately 153,020 individuals will receive a diagnosis of CRC, resulting in 52,550 deaths. Notably, this includes 19,550 cases and 3,750 deaths among individuals under the age of 50. The rate of decline in CRC incidence has slowed down, shifting from a significant decrease of 3-4% annually during the 2000s to a more modest 1% decline per year from 2011 to 2019.

This change is partly influenced by an increase in cases among individuals under the age of 55, which has been steadily rising at a rate of 1–2% yearly since the1990s. Notwithstanding the overall decline, there remains a concerning shift towards earlier onset, more advanced stages, and a tendency for the left colon and rectum in CRC cases(Seigel et al., 2023; Cisterna et al., 2016).Anticancer drugs for colon cancer targeting face significant challenges, such as suboptimal dosage delivery and off-target toxicities. Conventional administration methods lack selectivity toward colon cancer cells, limiting their effectiveness. To address this, site-specific drug delivery strategies have emerged (Mishra et al., 2023). By targeting the colon directly, these approaches aim to enhance drug concentration at the tumor site, minimizing systemic exposure and reducing side effects. Various techniques, including nanoparticles, prodrugs, and localized drug-release systems, have shown promise in improving drug efficacy while minimizing toxicity. Such advancements in colon cancer-targeted anticancer drug delivery hold great potential for enhancing treatment outcomes (Lee et al., 2020).Biodegradable polymer-based nanoparticles offer unique advantages in cancer treatment. They enable targeted drug delivery, reducing systemic toxicity. These nanoparticles can be engineered for controlled release, improving drug efficacy. Additionally, their biodegradability allows for safe elimination from the body, minimizing long-term side effects and improving patient outcomes (Jain et al., 2021; Pan et al., 2021).Biodegradable polymer-based nanoparticles, such as those incorporating hyaluronic acid (HyAc), polycaprolactone (PL), and polyethylene glycol (PEG), offer a promising approach for targeted drug delivery in colon cancer. HyAc targets CD44 receptors on colon cancer cells, facilitating specific drug delivery. PL provides sustained release properties, ensuring prolonged drug release at the target site (Gagliardi et al., 2021).PEG, a hydrophilic polymer, improves the stability and circulation time of nanoparticles, reducing clearance by the immune system and enhancing their accumulation in the colon. The combination of HyAc, PL, and PEG synergistically enhances the effectiveness of colon cancer treatment, minimizing off-target effects and improving therapeutic outcomes(Li et al., 2023; Prajapati et al. 2019).Doxorubicin (DX), a commonly utilized therapeutic agent, demonstrates significant efficacy in treating solid tumors affecting both pediatric and adult patients. Mechanistically, DX exerts its effects through intercalation within DNA base pairs, leading to DNA fragmentation and impeding the synthesis of DNA and RNA. Furthermore, DXinduced inhibition of topoisomerase II triggers DNA damage, consequently initiating apoptosis (Kciuk et al., 2023). In the present study, we designed formulation to enhance the therapeutic potential of DX by incorporating it into PL NPs and HyAc/PEG/PL NPs, while optimizing their composition. We subsequently evaluated the cytotoxicity of these novel DX-loaded nanoparticles in the HT-29 cell line, hemolytic toxicity, and their biodistribution. The primary objective of our planned investigation is to develop a safe and efficient treatment approach for colon cancer that minimizes adverse effects.

2. Materials and Methods

2.1 Materials

The HyAc and PL were delivered by Jay Appliance. Fresenius Kabi Ltd provided a free specimen of DX, while the procurement of Pluronic F-68 was made through a purchase from Sigma Aldrich in New Delhi, India. 1-ethyl-3-(3-dimethylaminopropyl) carbodiimide (EDC), acetonitrile, dimethyl sulfoxide (DMSO), DCM (Dichloromethane), ethylene diamine (EDA), NaOH, N-hydroxysuccinimide (NHS), and isopropyl alcohol were procured from Himedia Lab, Mumbai, India. PEG and dialysis sacs (MWCO 12000– 15000 Da) were delivered by Sigma Aldrich in New Delhi, India. The analytical grade was selected for all other compounds.

2.2. Methods of Preparation

2.2.1. Copolymer HyAc/PEG/PL Synthesis and Characterization

The exact quantity of HyAc and EDC was carefully weighed. Subsequently, the substances were dissolved in 10ml of DMSO. The resultant solution was subjected to stirring at ambient temperature for duration of 12 hours, thereby initiating activation of the carboxyl group within the HyAc

compound. Subsequent to this step, an additional solution comprising PEG, NHS, and DMSO, was introduced into the aforementioned solution. The mixture underwent ultrasonic agitation for duration of 5 minutes, followed by a reaction period of 24 hours. To eliminate byproduct, DMSO, and additional substances involved in the reaction, dialysis was conducted using buffer (PBS) and water. The HyAc/PEG conjugate was successfully synthesized by means of lyophilization. The resulting solid HyAc/PEG conjugate was then reacted with EDC, a coupling agent, in DMSO. EDC is a bifunctional molecule that can link two molecules together through an amide bond. In this case, EDC was used to link the HyAc/PEG conjugate to PL, a hydrophobic polymer. NHS, a co-reactant, was also added to the reaction mixture to promote the coupling reaction. DMSO was used as a solvent for all of the reactants. After the reactants were mixed, the mixture was sonicated for 5 minutes to facilitate the reaction. Once the reaction had been given 24 hours to proceed, the formation of the HyAc/PEG/PL conjugate would have occurred. After sonication, the reaction continued for 24 hours. Subsequently, a total of five dialysis cycles were carried out over a span of three days using a membrane and water as the medium to effectively eliminate DMSO and other residual reactants. The HyAc/PEG/PL conjugate was successfully obtained by subjecting the solution to lyophilization (Pang et al., 2021; Youm et al., 2014).

2.2.2. Preparation of DX-loaded HyAc/PEG/PL Nanoparticles (DX-HyAc/PEG/PL NPs)

Nanoprecipitation was employed as the chosen method to fabricate the DX-loaded NPs. At the beginning, a solution containing 100 mg of DX was dissolved in 6.2ml of NaOH and continuously stirred for 24 hours at room temperature (RT). Following this, a solution consisting of HyAc/PEG/PL copolymer (5 mg) in DCM (5 ml) was introduced into the DX solution while continuous stirring was maintained. In order to induce the formation of the NPs, the utilization of Pluronic F-68, a nonionic surfactant, was used. A solution comprising of Pluronic F-68 (10 ml) in distilled water was precisely prepared, and the organic solution containing the drug and polymer was integrated with the Pluronic F-68 solution. This resulting mixture was subjected to a stirring speed of 800 revolutions per minute (RPM) for a time frame of 24 hours, and subsequently subjected to a drying process, leading to the acquisition of the NPs. During the course of the experiment, the concentration of Pluronic F-68 remained unwaveringly constant at a level of 0.05% w/v, whereas the concentration of the copolymer exhibited variability ranging from 10 to 30 mg. Similarly, different concentrations of Pluronic F-68 were enlisted to produce NPs, with the proviso that the copolymer concentration remained constant at 10 mg (Yadav et al., 2008).

3. Characterization of Nanoparticles

3.1. Morphological Observation

The assessment of particle dimensions, polydispersity index, and zeta potential was conducted utilizing a Zetasizer apparatus manufactured by Malvern Instruments Ltd., situated in the United Kingdom. Themorphology of the NPs was examined using a transmission electron microscope (TEM) with an accelerating voltage of 200 kV. In preparation for TEM analysis, the samples were thoroughly placed on a copper grid coated with a layer of carbon, enabling the residual solvent to evaporate under normal light conditions (Jo et al., 2020).

3.2. Differential Scanning Calorimetry (DSC) Study

The crystal form was evaluated by performing DSC analysis on various samples, including pure PL, pure DX, a physical mixture of PL NPs, and DX-HyAc/PEG/PL NPs, using the TA Instrument 2910 MDSC V4.4E (Shin, Osaka, Japan). The heating procedure involved a gradual temperature increase at a rate of 5°C per minute, spanning from 40 to 400°C. A reference blank pan was employed, and a nitrogen gas purge was maintained to ensure an inert atmosphere (Anh et al., 2010).

3.3. X-ray Diffraction (XRD) Study

The analysis of the diffraction pattern of both developed formulation was performed using the X-ray diffractometer (Rigaku Denki Co. Ltd, Tokyo, Japan). To facilitate this investigation, Ni-filtered Cu-Kα radiation, known for its precision and reliability, was utilized.The experimental conditions were carefully controlled, maintaining a steady voltage of 35 kV and a current of 15 mA throughout the measurements. In order to capture a comprehensive understanding of the diffraction behavior, the temperature of the samples was intentionally varied within the temperature range of 0 to 50°C.By employing a voltage of 40 kV, the diffraction pattern of the samples was acquired(Guo et al., 2020).

3.4. DX Entrapment Efficiency (EE)

A solution containing of NP formulation (2 mg) was prepared by dissolving it in 2 ml of DMSO. Afterward, the suspension was subjected to sonication for 30 minutes, followed by centrifugation at a speed of 16,000 RPM for 10 minutes. The absorbance of the resulting supernatant was measured using a UV-Visible spectrophotometer, with a comparison made to a blank sample containing DMSO without the drug. By employing specific equations, the drug loading (DL) percentage and DL efficiency were determined (Soliman et al., 2019). To calculate the %EE, the following formula was applied:

EE% = (Amount of loaded drug / Total amount of drug) × 100%

3.5.In-Vitro Drug Release

In the evaluation of in-vitro release, a dialysis tube was utilized, employing two distinct release media: PBS at pH levels of 7.4 and 5.5. The experimental procedure involved dissolving a 2 ml NP formulation in 100 ml of the respective release media within dialysis tubing with MWCO ranging from 12,000 to 15,000 Da. To achieve complete mixing, a magnetic stirrer was adjusted to a constant speed of 100 RPM and maintained at a temperature of 37°C. Periodically, 1 ml of the release medium solution was removed and replaced with an equal volume of fresh medium. The measurement of the released drug was performed using a UV spectrophotometer (Thermo Scientific, Mumbai, India).

3.6. Cell Viability Study

With the use of the Sulforhodamine B (SRB) test, the vitality of the cells was examined. In RPMI 1640 medium that had fetal bovine serum (FBS 10%) and L-glutamine (2mm) added, HT-29 cells were grown.The cells were placed on 96-well microliter plates and subjected to precise environmental conditions (37°C, 95% air humidity, 100% relative humidity, and 5% CO2) for a 24 hours incubation period.The combination was then incubated for 48 hours with various formulations (DX-loaded PLNPs and DX-loaded HyAc/PEG/PL NPs) with the DX dosage of 20 g/ml, 40 g/ml, 60 g/ml, and 80 g/ml. A gentle addition of cold TCA (10% TCA) and an incubation period of 60 minutes at 4°C were used to fix the cells after discarding the supernatant and performing five consecutive water rinses, the plates were allowed to dry naturally. Subsequently, each well was filled with a 0.4% (w/v) SRB solution in acetic acid (1%), and the plates were incubated at room temperature for 20 minutes. The cells were stained, washed multiple times with acetic acid (1%) to remove any remaining unbound color, and then air dried. Absorbance measurements at 540 nm with a reference wavelength of 690 nm were taken using a plate reader (Bio-Rad, Model 550-Microplate Reader, Hercules, California) after the bound dye was eliminated using 10mM trizma base (Shalaby et al., 2016; Ortiz et al., 2015).

3.7. Hemolytic Toxicity Study

Vials made with the anticoagulant HiAnticlot by Himedia Labs were used to collect human blood. After being separated by centrifugation, the RBCs were immersed again in a sterile saline solution. The distilled water (regarded as the 100% hemolytic standard), normal saline (used as a blank for spectrophotometric estimation), DX, and DX-loaded HyAc/PEG/PL(200 mg/ml equivalent dose of DX) in a final volume of 10 ml using normal saline.After vigorous intermittent shaking for an hour at

37°C, the sample tubes were allowed to stand. Following this, the vials were centrifuged at 3000 RPM for 15 minutes, and the degree of hemolysis was evaluated by measuring the supernatant at 477 nm. This was established by comparing it to the absorbance of distilled water, which is considered 100% hemolytic when subjected to a similar dilution (Singh et al., 2020).The liquid fraction above the sediment was collected and subjected to spectrophotometric examination at the optimal wavelength (λ_{max}) subsequent to suitable dilution with normal saline. The proportion of erythrocyte lysis was determined utilizing the ensuing equation:

$$\text{Percentage of Hemolysis} = (Abs - Abs_0) / (Abs_{100} - Abs_0) \times 100$$

Here, Abs denotes the absorbance of the analyzed samples, Abs_0 represents the absorbance of a solution devoid of any hemolysis (0% hemolysis), and Abs_{100} signifies the absorbance of a solution with complete hemolysis (100% hemolysis).

3.8. Biodistribution Study

The animals were categorized into three groups, and following the administration of the formulations, they were sacrificed at 3 different time point: one hour, six hours, and twenty-fourhours. Afterwards, the visceral organs, such as the colon, lungs, liver, kidney, and tumor were meticulously separated, washed twice to eliminate any attached cell debris or tissues, and preserved in frozen conditions. These tissue samples were homogenized and agitated in pH 7.4 PBS using a Superfit instrument manufactured in Mumbai, India. Subsequently, the homogenates underwent centrifugation at 30,000 RPM for 15 minutes, and the resulting supernatant was collected in a clean, dry vial. The contents were then subjected to treatment with a 10% TCA solution, followed by vortexing, centrifugation, and filtration utilizing a Millipore system from Billerica, MA. Finally, the obtained clear supernatant was analyzed using the HPLC method without the inclusion of any internal standard.

3.9. Stability Study

The stability of the PL NPs and HyAc/PEG/PL NPs was evaluated for a period of 180 days at room temperature (28°C) and under refrigeration (4±2°C; R-26SVND, Hitachi, Tokyo, Japan). Throughout the study period, the samples were periodically analyzed for changes in particle size and %EE at specific time points (15, 30, 60, 90, 150, and 180 days). Additionally, after three months, an examination was conducted to identify any alterations in the sample's color, remaining drug content.

4. Statistical Analysis

The statistical analysis was performed using GraphPadInstat Software (Version 3.00, Graph Pad Software, San Diego, CA). To compare multiple groups, Tukey-Kramer tests were employed following a one-way ANOVA. A significance level of $p \leq 0.05$ was chosen as the threshold for determining statistical significance. The experimental results were presented as the mean ± standard deviation (S.D.).

5. Results and Discussion

The management of cancer has always posed significant challenges, primarily due to the associated drawbacks of conventional treatments. However, an emerging field of research utilizing nanotechnology-based approaches has gained considerable traction due to its potential to minimize adverse effects. In this particular investigation, the researchers employed a combination of biodegradable polymers, namely HyAc, PL, and PEG, along with PL alone, to develop nanoparticles. These selected polymers are renowned for their biodegradable and biocompatible properties, as well as their ability to specifically target cancer cells, as highlighted in prior studies by Prajapati et al. (2019) and Quindeel et al. (2020).To evaluate the potential of NPs for the treatment of cancer, DX-loaded NPs was developed by nanoprecipitation method. Subsequently, the formulations were characterized in terms of their particle size, surface morphology, and effectiveness in encapsulating DX. The DX-loaded

NPs were optimized by adjusting the concentration of the copolymer, the concentration of the surfactant, the stirring time, and the stirring speed. By varying the copolymer concentration while keeping the other factors constant, the NPs were successfully created. The influence of the copolymer concentration on particle size and %EE (percentage of encapsulation efficiency) was clearly observed. When 10 mg of copolymer was used, the NPs exhibited maximum %EE (87.5±2.7 nm) and optimal size (130±2.1 nm). This could be attributed to particle aggregation, as increasing the concentration did not further affect the %EE. At the lowest copolymer concentration (5 mg), the average particle size was 152±2.4 nm, with a %EE of 75.3±1.5%.While the other factors remained unchanged, the concentration of the surfactant had a significant impact on the %EE and particle size. Increasing the surfactant concentration from 0.5% to 1.0% resulted in a reduction in particle size from 181±2.2 nm to 148±2.8 nm. Achieving an optimal surfactant concentration of 1.5% led to a desirable size of 148±2.8 nm and %EE of 87.3±2.4%.At a stirring speed of 500 RPM, the ideal particle size was found to be 189±1.8 nm, with a %EE of 86.10±1.1%. However, due to particle aggregation, an increase in stirring speed from 200 to 700 RPM caused an increase in particle size. The maximum %EE of 92.16±2.3% and particle size of 267±2.0 nm was achieved when the formulation was stirred for 12 hours, indicating successful optimization of the stirring period. The summarized optimized data is presented in Table 1.

Table 1: Optimization of process and formulation variables in preparation of nanoparticles

Formulation Code	Copolymer Conc. (%)	Drug Conc. (mg)	Surfactant Conc. (%)	Stirring Speed	Stirring Time (hours)	EE (%)	Average Particle Size (nm)
Copolymer Concentration							
F1P1	5	100	0.5 %	500	6	75.3±1.5	152±2.4
F2P2	10	100	0.5 %	500	6	87.5±2.7	130±2.1
F3P3	15	100	0.5 %	500	6	83.3±1.2	178±6.1
Surfactant Concentration							
F1S1	10	100	0.5 %	500	6	73.3±1.6	181±2.2
F1S2	10	100	1 %	500	6	81.5±2.8	162±2.5
F1S3	10	100	1.5 %	500	6	87.3±2.4	148±2.8
Stirring Speed							
F1S3R1	10	100	1.5 %	250	6	70.05±1.1	173±2.2
F1S3R2	10	100	1.5 %	500	6	86.10±1.6	189±1.8
F1S3R3	10	100	1.5 %	700	6	89.13±1.3	204±2.5
Stirring Time							
F1S3R2T1	10	100	1.5 %	500	6	71.02±1.3	272±2.0
F1S3R2T2	10	100	1.5 %	500	12	92.16±2.3	267±2.0
F1S3R2T3	10	100	1.5 %	500	24	76.41±1.6	191±1.4

Table 2: Particle size, zeta potential and PDI

Formulation Code	Particle Size (nm)	Zeta Potential (mV)	PDI
HyAc/PEG/PL NPs	268±3nm	-16.4±0.8 mV	0.648
PL NPs	142±1.5nm	-4.9±0.3mV	0.553

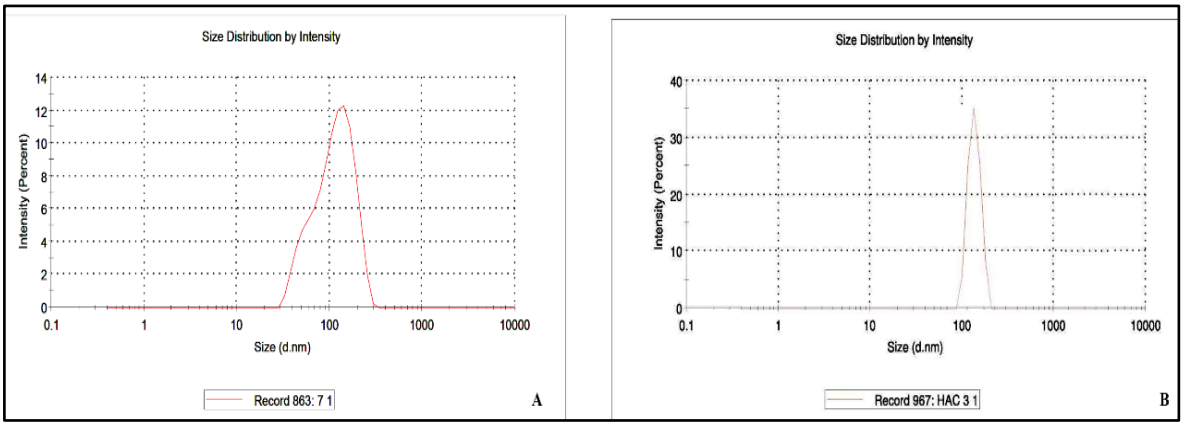

Figure 1: Particle size of (A) HyAc/PEG/PL NPs and (B) PL NPs measured by zeta sizer

5.1. TEM of Formulations

The findings from the TEM examinations of the developed formulations (as shown in Figure 2) confirmed that the NPs possessed a shape that closely resembled a sphere, and their size distribution was tightly controlled. This means that the NPs exhibited a uniform and consistent spherical shape, which is desirable for many applications. The TEM image provided visual evidence of the particle size. This measurement was obtained by directly observing the particles using the TEM technique, which allows for high-resolution imaging at the nanoscale.However, when the average particle size was determined using the zeta sizer method, a slightly larger size was obtained compared to the TEM measurement. The zeta sizer technique measures the hydrodynamic diameter of solid structures, which includes not only the solid core of the NPs but also the layer of solvent molecules or other substances surrounding them. This hydrodynamic layer affects the overall size measurement obtained by the zeta sizer method.

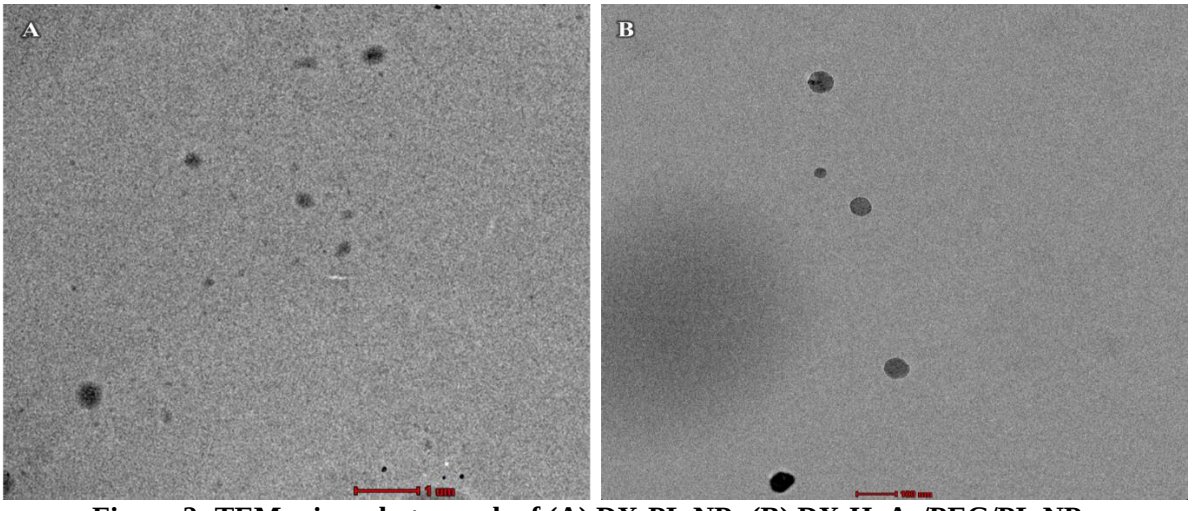

Figure 2: TEM microphotograph of (A) DX-PL NPs (B) DX-HyAc/PEG/PL NPs

5.2. DSC Analysis

DSC analysis greatly facilitated the examination of thermal properties of NPs and provided qualitative and quantitative data on the physicochemical state of drugs and drug combinations. Figure 3 illustrates a DSC Thermogram showing HyAc/PEG/PL NPs and PL NPs loaded with DX, HyAc, PL, diamine PEG, and PL. The endothermic peak of DX was observed at 105°C, while diamine PEG exhibited a strong peak at 69°C, and PL displayed an endothermic peak at 61°C, corresponding to their respective melting points. H displayed a significant peak at 311.2°C, confirming the crystalline composition of the excipients. DX-loaded HyAc/PEG/PL NPs exhibited sharp endothermic peaks at 99°C, 510°C, and

69°C, while PL in DX-loaded PL NPs demonstrated a peak at 60°C (Yadav et al., 2008; Quindeel et al., 2020).

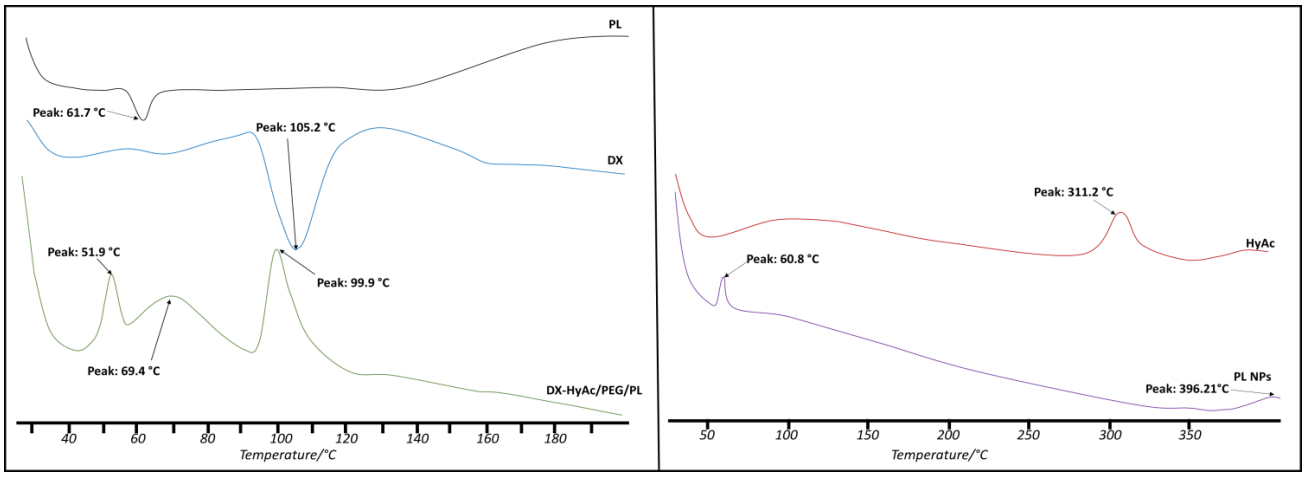

Figure 3: DSC thermogram of PL, FreeDX, HyAc, DX-HyAc/PEG/PL NPs,PL NPs

5.3. XRD Analysis

The XRD patterns depicted in Figure 4 illustrate the XRD of DX,PL NPs and DX-Loaded HyAc/PEG/PL NPs. The XRD patterns of DX displayed distinct sharp peaks, signifying their crystalline character. The utilization of HyAc/PEG/PLcopolymers may have effectively regulated the prolonged degradation durations of PL, a hydrophobic semi-crystalline polymer, leading to improved physicochemical attributes and process ability. The analysis of XRD peaks in HyAc/PEG/PL NPs provided evidence of the copolymer's crystalline composition. Contrasting the relatively fewer peaks observed in blank NPs, the XRD patterns of DX-loaded HyAc/PEG/PL NPs exhibited the distinct sharp peaks associated with the drug crystal. Notably, the XRD patterns of DX-loaded HyAc/PEG/PL NPs clearly displayed unique peaks corresponding to the drug.

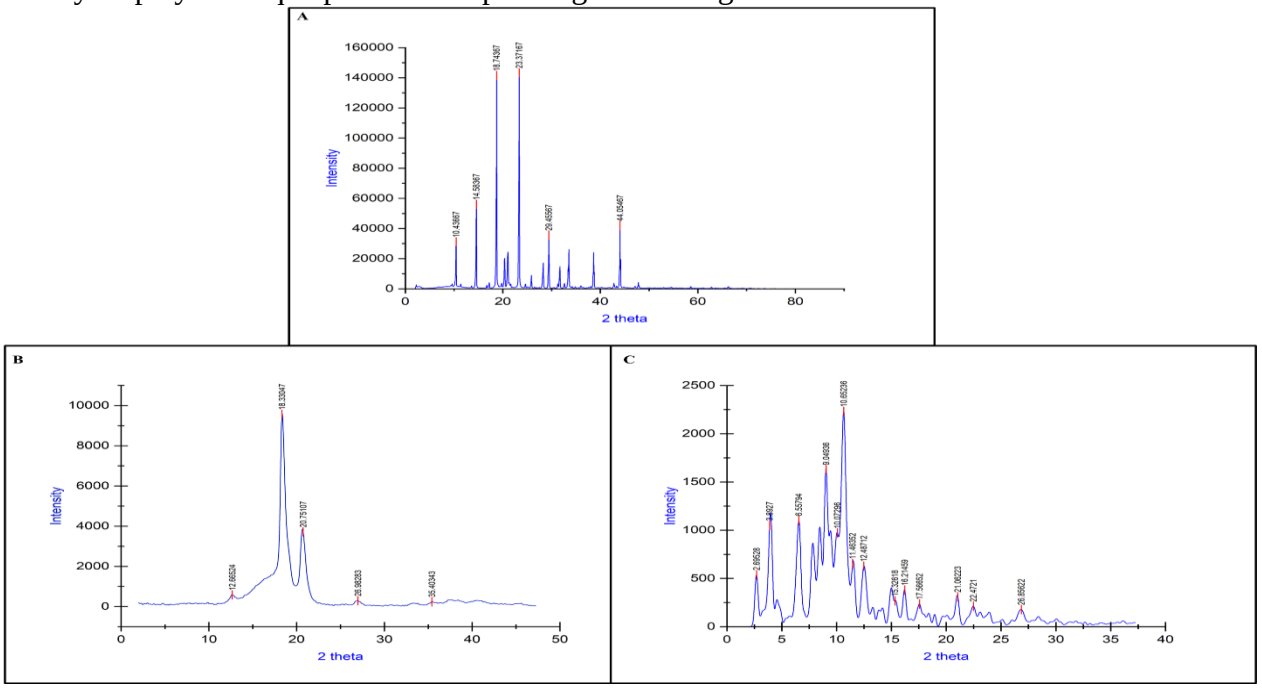

Figure 4: XRD of (A) DX (B) PL NPs, (C) DX-HyAc/PEG/PL NPs

5.4. In Vitro Drug Release

The release behavior of DX from HyAc/PEG/PL copolymer-prepared NPs was investigated, and the results are presented in Figure 5. The NPs exhibited a sustained release profile, indicating their capacity to control the release of DX over time. Initially, a burst release of the drug was observed, which could be attributed to the presence of surface-adsorbed medication on the NPs.The release of DX was found to be influenced by the environmental acidity, with a slower release rate observed at pH 5.5 compared to pH 7.4. This pH-dependent behavior can be attributed to the physicochemical properties of DX and its interaction with the copolymer matrix.In comparison to DX-loaded PL NPs, DX-loaded HyAc/PEG/PL NPs demonstrated higher release efficiency, with approximately 96.7±2.3% of the drug released within 144 hours at pH 7.4 and 98.8±3.1% at pH 5.5. On the other hand, DX-loaded PL NPs released approximately 99.2±2.2% of the drug within 120 hours at pH 7.4 and 91.4±1.61% within 144 hours at pH 5.5.The hydrophobic nature of DX, combined with its entrapment within the inner core of the co polymeric NPs, contributed to the controlled and sustained release profile observed. The design of these NPs aimed to minimize their uptake by the reticuloendothelial system (RES), which allowed for an extended circulation time in the bloodstream. This strategy enhances the therapeutic efficacy of DX by ensuring a prolonged exposure to the targeted site while reducing potential side effects associated with rapid drug clearance (Yoshida et al., 2013; Chang et al., 2020).The HyAc/PEG/PL copolymer-based NPs demonstrated their capability to sustain the release of DX, offering controlled drug delivery behavior influenced by environmental pH and designed to improve therapeutic outcomes.

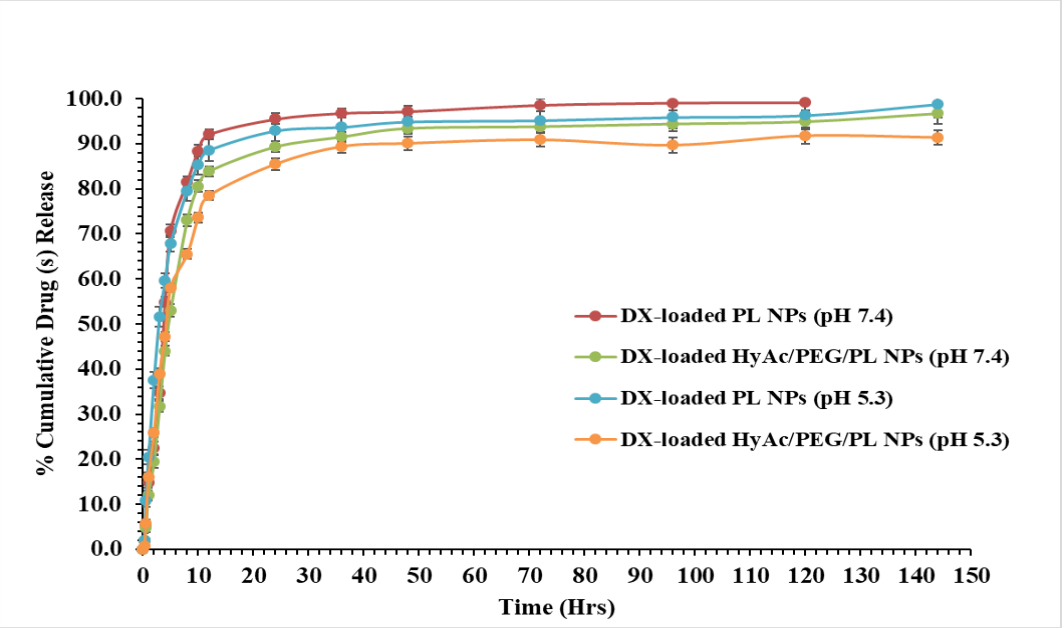

Figure 5:In Vitro DX release from PL NPs andHyAc/PEG/PLNPs at pH 7.4 and 5.3

5.5. Cell viability

The study conducted on cell lines showed interesting results, as presented in Figure 6. It was evident that DX-loaded HyAc/PEG/PL NPs exhibited significantly greater cytotoxicity when compared to free DX and DX-loaded PL after a 72hours exposure to the cells. Notably, at a dosage of 0.01 mg/ml, free DX displayed minimal cytotoxicity, inhibiting the proliferation of only 59.5±1.5% of the cells. This outcome could be attributed to inadequate absorption of the drug by the cells, thereby limiting its effectiveness. Similarly, DX-loaded PL NPs demonstrated a relatively lower inhibitory effect on cell growth, with a 45.3±1.4% decrease observed. This could be attributed to factors such as passive diffusion, restricted intracellular dispersion, or suboptimal drug concentration within the cells. In

contrast, DX-loaded HyAc/PEG/PL NPs exhibited a higher inhibition of cell growth, approximately 20.6±1.2%. This enhanced cytotoxicity can be attributed to the internalization of the formulation through HyAc receptor-mediated endocytosis, facilitated by the presence of HyAc as a ligand. It is noteworthy that CD44 receptors, which are over expressed on HT-29 cells, the cell line used in this study, have a specific affinity for HyAc. Consequently, the incorporation of HyAc polymer in the formulation (DX-HyAc/PEG/PL NPs) likely facilitated improved internalization and enhanced cytotoxicity (Manjili et al., 2016; Norouzi et al., 2020). The data indicated that cell viability was relatively higher at lower concentrations of the formulations, while a noticeable increase in cytotoxicity was observed with escalating concentrations. These findings emphasize the potential of the DX-loaded HyAc/PEG/PL NP formulation as a promising approach for targeted cancer therapy.

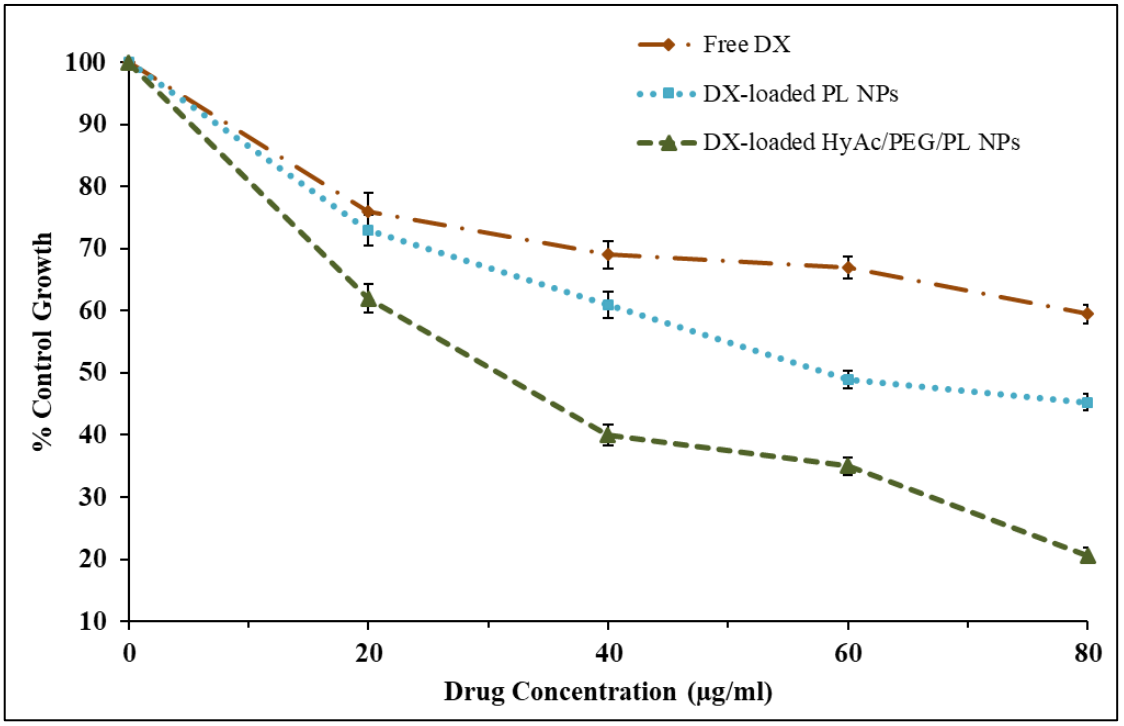

Figure 6: Percent cell growth inhibition by DX, DX-loaded PLNPs and DX-loaded HyAc/PEG/PLNPs

5.6. Hemolytic Toxicity Study

The extent of hemolytic toxicity caused by DX varies depending on its concentration. No hemolysis was observed at concentrations below 100 mg/ml however, at a concentration of 200 mg/ml, it resulted in 11% hemolysis. Hemolytic assays were performed on red blood cells (RBCs) to evaluate the hemolytic activities of both free DX and DX-loaded HyAc/PEG/PLNPs. The formulations of DX-loaded HyAc/PEG/PLNPs demonstrated minimal hemolytic toxicity on RBCs, even at the concentration of 200 mg/ml utilized in the experiments. These findings indicate the high hemocompatibility of DX-loaded HyAc/PEG/PLNPs for applications in drug delivery. The observed suppression of hemolytic toxicities is consistent with previous studies conducted on PEG/PL micelles (Figure 7)(Yadav et al., 2008; Singh et al., 2020; Li et al., 2020).

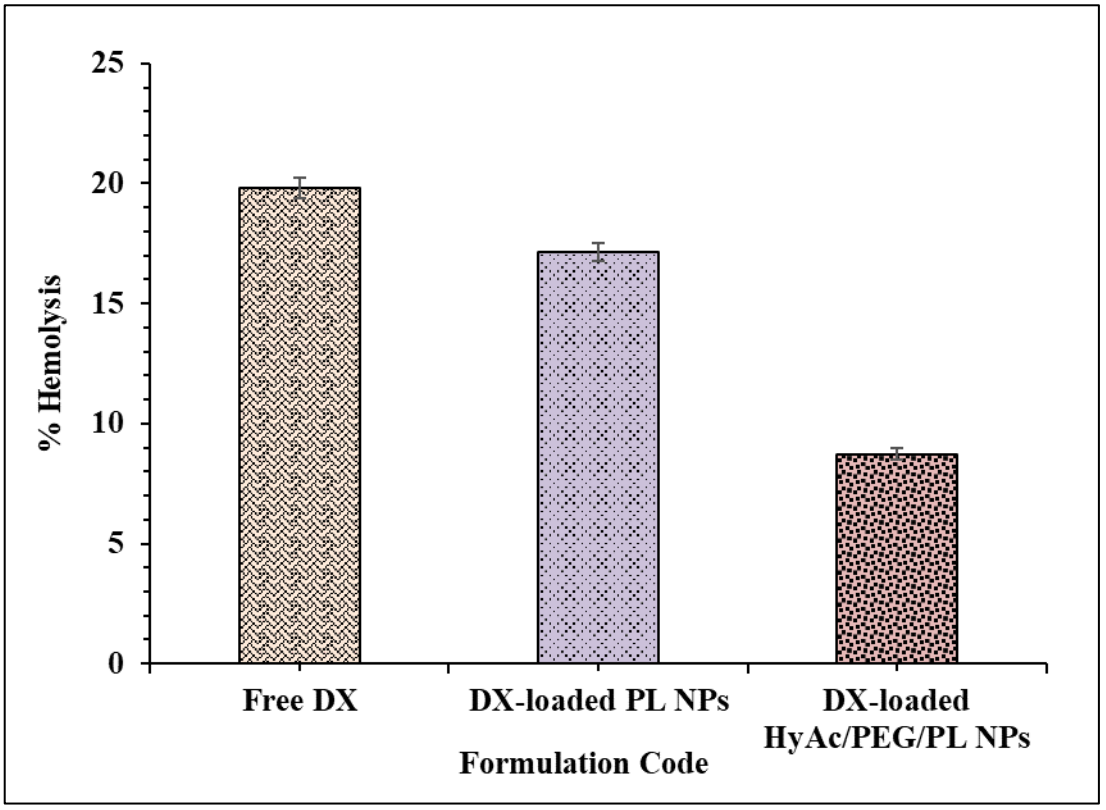

Figure 7: Hemolytic Toxicity of Free DX, DX-loaded PL NPs and DX-loaded HyAc/PEG/PLNPs

5.7. Tissue Distribution Analysis

Following the administration of different formulations including DX, DX-loaded PL NPs, and DX-loaded HyAc/PEG/PLNPs, the concentration of DX was monitored for 24 hours. The analysis revealed that DX concentrations in the lung, liver, kidney, colon, and tumor after 24 hours were as follows: 1.01±0.011%, 6.58±0.25%, 9.35±0.19%, 1.23±0.005%, and 3.9±0.25% for DX solution, 4.35±0.93%, 1.8±0.096%, 4.85±0.17%, 14.9±0.93%, and 14.74±0.89% for DX-loaded PL NPs, and 9.87±0.62%, 6.58±0.18%, 7.21±0.42%, 17.54±0.85%, and 14.74±0.89% for DX-loaded HyAc/PEG/PL NPs (Figure 8). Notably, DX-loaded HyAc/PEG/PL NPs exhibited significantly higher concentrations of DX in the colon and tumor compared to free DX solution and DX-loaded PL NPs. Moreover, both NP formulations reduced the accumulation of DX in the liver. This effect could be attributed to the abundant presence of HyAc receptors on colon cancer cells. PEGylation of the NPs effectively slowed down the liver's uptake of DX-loaded PL NPs and DX-loaded HyAc/PEG/PL NPs, while enhancing their circulation in the bloodstream (Jain& Yadav 2023).

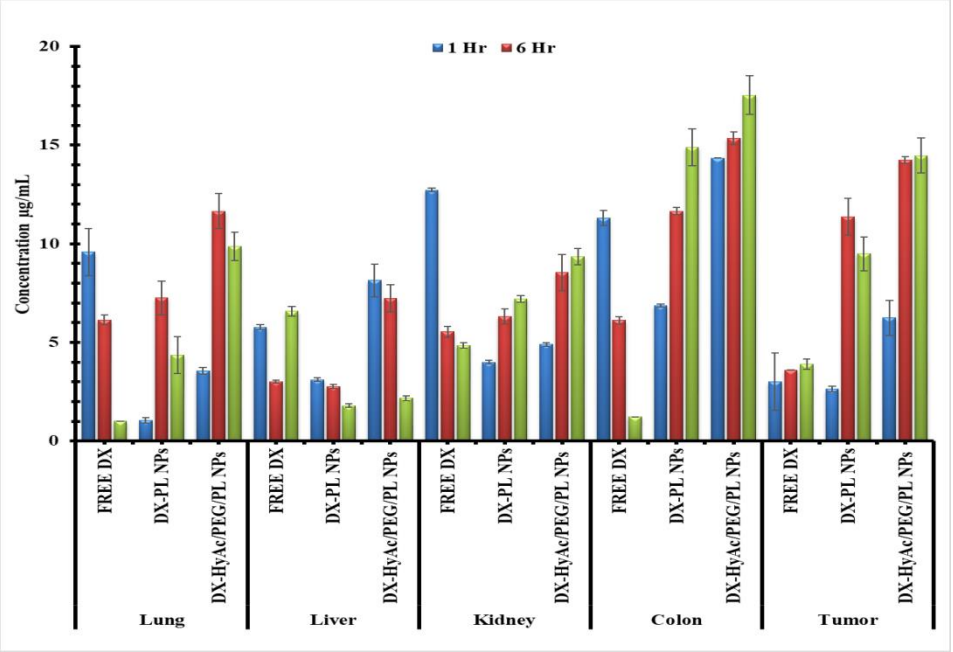

Figure 8: Tissue Distribution study of DX, DX-loaded PL NPs and DX-loaded HyAc/PEG/PL NPs after IV administration

5.8. Stability

The DX-loaded PL NPs formulation exhibited a gradual decrease in drug content over time at both temperature conditions. At 4±2°C, the decrease was relatively stable, with a decrease of around 3.5% over the course of 180 days. However, at 28±2°C, there was a more significant reduction in drug content, reaching 13.5% after 180 days. The higher temperature likely accelerated the degradation of the DX-loaded PL NPs, leading to a more pronounced decline in drug content. The DX-loaded HyAc/PEG/PL NPs formulation demonstrated relatively higher stability compared to the DX-loaded PL NPs formulation. At 4±2°C, the decrease in drug content was gradual, with a decline of approximately 3.2% over 180 days. However, at 28±2°C, the formulation experienced a more significant reduction in drug content, showing a decrease of 10.2% after 180 days. The presence of hyaluronic acid and PEG in the formulation likely contributed to enhanced stability compared to the DX-loaded PL NPs, but the higher temperature still had a notable impact on the degradation of the DX-loaded HyAc/PEG/PL NPs. During the evaluation, it was observed that the drug content exhibited a decline at 28±2°C, potentially attributed to certain factors influencing its stability. This decrease in drug content may be attributed to factors such as environmental conditions, drug physicochemical properties, or interactions within the formulation itself. In contrast, at 4±2°C, no significant changes in the drug content were noted, indicating a higher level of stability at this lower temperature. Furthermore there may be indications of drug leakage or degradation, potentially compromising the efficacy of the formulation (Figure 9).

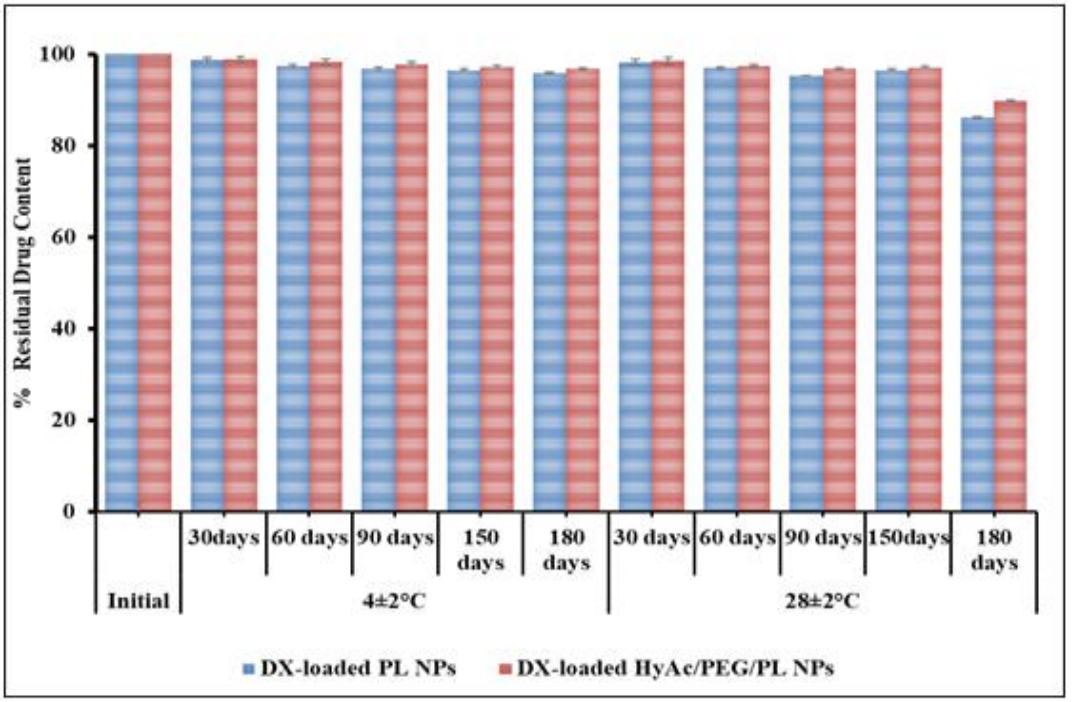

Figure 9: Effect of storage at 4±2^{0}C and 28±2^{0}C

6. Conclusion

In conclusion, our study focused on enhancing the therapeutic potential of doxorubicin (DX) by formulating it into PL NPs and HyAc/PEG/PL NPs while optimizing their composition. The primary objective was to develop a safe and efficient treatment approach for colon cancer, aiming to minimize adverse effects. By utilizing a combination of biodegradable polymers, including HyAc, PL, and PEG, we successfully developed NPs with desirable physicochemical properties. The optimized NPs exhibited controlled and sustained release of DX, indicating their potential for improved therapeutic outcomes. The hemolytic toxicity assay demonstrated the high hemocompatibility of DX-loaded HyAc/PEG/PL NPs. The cytotoxicity of these novels DX-loaded NPs was evaluated in the HT-29 cell line. Moreover, biodistribution analysis revealed higher concentrations of DX in the colon and tumor when delivered using DX-loaded HyAc/PEG/PL NPs, suggesting enhanced targeting ability. Findings support the potential of these novel NPs as a promising approach for targeted cancer therapy, offering improved therapeutic outcomes while minimizing adverse effects.

Declaration of interest

No conflicts of interest.

References

Anh Nguyen, T. H., & Nguyen, V. C. (2010). Formation of nanoparticles in aqueous solution from poly (ε-caprolactone)–poly (ethylene glycol)–poly (ε-caprolactone). Advances in Natural Sciences: Nanoscience and Nanotechnology, 1(2), 025012.

Chang, N., Zhao, Y., Ge, N., & Qian, L. (2020). A pH/ROS cascade-responsive and self-accelerating drug release nanosystem for the targeted treatment of multi-drug-resistant colon cancer. Drug Delivery, 27(1), 1073-1086.

Cisterna, B. A., Kamaly, N., Choi, W. I., Tavakkoli, A., Farokhzad, O. C., &Vilos, C. (2016). Targeted nanoparticles for colorectal cancer. Nanomedicine, 11(18), 2443-2456.

Gagliardi, A., Giuliano, E., Venkateswararao, E., Fresta, M., Bulotta, S., Awasthi, V., &Cosco, D.

(2021). Biodegradable polymeric nanoparticles for drug delivery to solid tumors. Frontiers in pharmacology, 12, 601626.

Guo, Q., Kong, F., Ma, C., & Cao, H. (2020). Preparation of doxorubicin loaded Poly (ethylene glycol)-Poly (ε-caprolactone)-hydroxyapatite fibres as drug delivery systems. Materials Technology, 35(4), 203-211.

Jain, A., Tripathi, M., Prajapati, S. K., & Raichur, A. M. (2021). Biopolymer Matrix Composite for Drug Delivery Applications in Cancer. 804-817.

Jain, D., & Yadav, A. K. (2023). Development of hyaluronic acid–anchored polycaprolactone nanoparticles for efficient delivery of PLK1 siRNA to breast cancer. Drug Delivery and Translational Research, 1-15.

Jo, Y. U., Lee, C. B., Bae, S. K., & Na, K. (2020). Acetylated hyaluronic acid-poly (L-lactic acid) conjugate nanoparticles for inhibition of Doxorubicinol production from Doxorubicin. Macromolecular Research, 28(1), 67-73.

Kciuk, M., Gielecińska, A., Mujwar, S., Kołat, D., Kałuzińska-Kołat, Ż., Celik, I., &Kontek, R. (2023). Doxorubicin-An Agent with Multiple Mechanisms of Anticancer Activity. Cells, 12(4), 659.

Lee, S. H., Bajracharya, R., Min, J. Y., Han, J. W., Park, B. J., & Han, H. K. (2020). Strategic approaches for colon targeted drug delivery: an overview of recent advancements. Pharmaceutics, 12(1), 68.

Li, K., Zhan, W., Jia, M., Zhao, Y., Liu, Y., Jha, R. K., & Zhou, L. (2020). Dual loading of nanoparticles with doxorubicin and icotinib for the synergistic suppression of non-small cell lung cancer. International Journal of Medical Sciences, 17(3), 390.

Li, M., Liu, Y., &Weigmann, B. (2023). Biodegradable Polymeric Nanoparticles Loaded with Flavonoids: A Promising Therapy for Inflammatory Bowel Disease. International Journal of Molecular Sciences, 24(5), 4454.

Manjili, H. K., Sharafi, A., Danafar, H., Hosseini, M., Ramazani, A., &Ghasemi, M. H. (2016). Poly (caprolactone)–poly (ethylene glycol)–poly (caprolactone)(PCL–PEG–PCL) nanoparticles: a valuable and efficient system for in vitro and in vivo delivery of curcumin. Rsc Advances, 6(17), 14403-14415.

Mishra, N, Garg A, Upmanyu N, editors. Therapeutic Nanocarriers in Cancer Treatment: Challenges and Future Perspective. Bentham Science Publishers; 2023 Mar 6.

Norouzi, M., Yathindranath, V., Thliveris, J. A., Kopec, B. M., Siahaan, T. J., & Miller, D. W. (2020). Doxorubicin-loaded iron oxide nanoparticles for glioblastoma therapy: A combinational approach for enhanced delivery of nanoparticles. Scientific reports, 10(1), 11292.

Ortiz, R., Cabeza, L., Arias, J. L., Melguizo, C., Álvarez, P. J., Vélez, C., ... & Prados, J. (2015). Poly (butylcyanoacrylate) and poly (ε-caprolactone) nanoparticles loaded with 5-fluorouracil increase the cytotoxic effect of the drug in experimental colon cancer. The AAPS journal, 17, 918-929.

Pan, D. C., Krishnan, V., Salinas, A. K., Kim, J., Sun, T., Ravid, S., ... &Mitragotri, S. (2021). Hyaluronic a cid–Doxorubicin nanoparticles for targeted treatment of colorectal cancer. Bioengineering & Translational Medicine, 6(1), e10166.

Pang, L., Zhong, W., Wang, Q., Feng, H., Dong, H., Wang, S., ... & Yu, B. (2021). Preparation and anti-tumor application of hyaluronic acid-based material for disulfide and copper ions co-delivery. Science China Technological Sciences, 64(9), 2023-2032.

Prajapati, S. K., Jain, A., Shrivastava, C., & Jain, A. K. (2019). Hyaluronic acid conjugated multi-walled carbon nanotubes for colon cancer targeting. International journal of biological macromolecules, 123, 691-703.

Qindeel, M., Ahmed, N., Shah, K. U., & Ullah, N. (2020). New, environment friendly approach for synthesis of amphiphilic PCL–PEG–PCL triblock copolymer: an efficient carrier for fabrication of nanomicelles. Journal of Polymers and the Environment, 28, 1237-1251.

Shalaby, K. S., Soliman, M. E., Bonacucina, G., Cespi, M., Palmieri, G. F., Sammour, O. A., ...

&Casettari, L. (2016). Nanoparticles based on linear and star-shaped poly (ethylene glycol)-poly (ε-caprolactone) copolymers for the delivery of antitubulin drug. Pharmaceutical Research, 33, 2010-2024.

Siegel, R. L., Miller, K. D., Wagle, N. S., Jemal, A. Cancer statistics, 2023. CA: a cancer journal for clinicians. 2023 Jan;73(1):17-48.

Singh, N., Sahoo, S. K., & Kumar, R. (2020). Hemolysis tendency of anticancer nanoparticles changes with type of blood group antigen: An insight into blood nanoparticle interactions. Materials Science and Engineering: C, 109, 110645.

Soliman, S. M. A., El Founi, M., Vanderesse, R., Acherar, S., Ferji, K., Babin, J., & Six, J. L. (2019). Light-sensitive dextran-covered PNBA nanoparticles to continuously or discontinuously improve the drug release. Colloids and Surfaces B: Biointerfaces, 182, 110393.

Yadav, A. K., Mishra, P., Jain, S., Mishra, P., Mishra, A. K., & Agrawal, G. P. (2008). Preparation and characterization of HA–PEG–PCL intelligent core–corona nanoparticles for delivery of doxoorubicin. Journal of drug targeting, 16(6), 464-478.

Yoshida, T., Lai, T. C., Kwon, G. S., &Sako, K. (2013). pH-and ion-sensitive polymers for drug delivery. Expert opinion on drug delivery, 10(11), 1497-1513.

Youm, I., Agrahari, V., Murowchick, J. B., &Youan, B. B. C. (2014). Uptake and cytotoxicity of docetaxel-loaded hyaluronic acid-grafted oily core nanocapsules in MDA-MB 231 cancer cells. Pharmaceutical research, 31, 2439-2452.